

The nominal noise temperature brought to the maser input does not exceed 25° K.

## V. CONCLUSION

Thus, our efforts have resulted in the implementation of a millimeter-range traveling-wave maser using andalusite which at the moment of work completion was the shortest-wavelength maser of its type.

Recently, we have become aware of a rutile maser operating at even shorter wavelengths [12].

Currently, our maser is the most wide-band TWM of the millimeter range supposedly to become useful for spectral and radiometric applications.

The physical results obtained suggest the possibility of a further extension of the amplification band, to several hundred megahertz, and shortening of the operation wavelength to  $\lambda < 3$  mm.

Since the end of 1981, the maser has been employed as an amplifier in the radio telescope RT-25×2 (Institute for Applied Physics, Academy of Sciences of the U.S.S.R., Gorky).

## ACKNOWLEDGMENT

The authors wish to express their gratitude to L. I. Fedoseev (Institute for Applied Physics, Academy of Sciences of the U.S.S.R.) who has developed the Zender-Mach interferometer placed at our disposal by courtesy of Dr. A. G. Kislyakov.

It is a pleasure to thank Dr. E. L. Kollberg of the Chalmers University of Technology in Göteborg, Sweden for having sent us a technical report on the rutile traveling-wave maser.

## REFERENCES

- [1] N. T. Cherpak, "Cross relaxation in inverted spin system of three-valence iron ions in andalusite," *Solid State Phys. (Fizika Tverdogo Tela, USSR)*, vol. 22, pp. 3539-3543, Dec. 1980 (in Russian).
- [2] N. T. Cherpak, A. A. Lavrinovich, V. V. Mishchenko, and T. A. Smirnova, "Investigation of comb-type retarding structure for millimeter-band maser," *Radioelectron. and Communicat. Syst. (Izv. VUZ Radioelectron., USSR)*, vol. 24, pp. 9-14, December, 1981 (in Russian).
- [3] V. I. Ivanova, L. N. Kolpakova, I. I. Petrova, T. A. Smirnova, and N. T. Cherpak, "Investigation of hexagonal ferrites  $Ni_2Sc_xW$  by FMR method throughout the temperature range 300-4.2° K," *Magnetic Resonance and Related Phenomena* (Proc. XXth Congr. Ampere, Tallinn, USSR, Aug. 21-26, 1978). Berlin, Heidelberg, New York: Springer, 1979, p. 371.
- [4] N. T. Cherpak, V. V. Mishchenko, S. A. Peskovskii, and T. A. Smirnova, "Andalusite traveling-wave maser in the millimeter wavelength range," *Dokl. Akad. Nauk Ukr. SSR* (in Russian), ser. A, pp. 69-71, Feb. 1980.
- [5] N. T. Cherpak, T. A. Smirnova, V. V. Mishchenko, S. A. Peskovskii, and A. A. Lavrinovich, "Traveling wave maser in 6-mm wave band with instantaneous bandwidth exceeding 100 MGz," in *III All-Union Sym. Millimeter and Submillimeter Waves*, September, 22-24, 1980, Gorky, Inst. Applied Phys., Acad. Sciences of the USSR, 1980, pp. 23-24.
- [6] L. I. Marchenko, V. V. Mishchenko and N. T. Cherpak, "Broad-band matching in the traveling-wave paramagnetic amplifier," *Radioelectron. and Communicat. Syst. (Izv. VUZ Radioelectron., USSR)*, vol. 22, pp. 75-76, Sept. 1979 (in Russian).
- [7] L. I. Fedoseev and Yu. Yu. Kukhov, "Superheterodyne radiometers of millimeter and submillimeter wavebands," *Radio Eng. El. Phys. (Radio-tehnika i elektron., USSR)*, vol. 16, pp. 554-560, Apr. 1971, (in Russian).
- [8] V. P. Shestopalov, *Difraktsionnaja Elektronika*. Kharkov: State University, 1976 (in Russian).
- [9] V. I. Zagatin, G. A. Misezhnikov, and V. B. Shteinglyer, "Ruby maser operating in the 8-mm range," *Radio Eng. El. Phys.*, vol. 12, pp. 501-502, Mar. 1967.
- [10] E. L. Kollberg and P. Th. Lewin, "Traveling wave masers for radio astronomy in the frequency range 20-40 GHz," *IEEE Trans. Microwave Theory Tech.*, vol. MTT-22, pp. 718-725, Nov. 1976.
- [11] N. T. Cherpak, "Amplification and absorption of an electromagnetic wave in slowing structure with a paramagnetic crystal," *Izv. VUZ Radiofizika (USSR)*, vol. 22, pp. 819-825, July 1979 (in Russian).
- [12] T. C. L. G. Sollner, D. P. Clemens, T. L. Korzeniowski, G. C. McIntosh, E. L. Moor, and K. S. Yngvesson, "Low-noise 86-88 GHz traveling wave maser," *Appl. Phys. Lett.*, vol. 35, pp. 833-835, Nov. 1979.

## A Note Concerning Modes in Dielectric Waveguide Gratings for Filter Applications

GEORGE L. MATTHAEI, FELLOW, IEEE

**Abstract**—Peng and Oliner, and others have shown that TM-to-TE or TE-to-TM mode conversions occur when a single, lowest order surface wave is incident obliquely onto a wide dielectric grating and that the lowest order converted modes of this sort can cause spurious stopbands which are especially troublesome because they are so close to the desired stopband. In this note it is observed that the spurious response situation is not as bad in the case of a grating cut into a dielectric waveguide (which can be thought of as having two, obliquely incident waves present). In this latter case, the fields have even or odd symmetry which eliminates part of the mode couplings including the lowest order TM-to-TE or TE-to-TM couplings. Experimental and theoretical results indicate that gratings can be made to be free from spurious responses or appreciable radiation over sizeable bands so that they can be useful in at least some kinds of dielectric waveguide filter structures.

## I. BACKGROUND

Peng, Oliner, and their coauthors have made extensive studies of propagation effects in dielectric waveguides [1], [2]. In particular, they show that TE-to-TM (or TM-to-TE) mode conversion at the side walls of a uniform guide can result in leakage and other effects not apparent from the often used approximate theories. In this context it should be noted that by a "TE" mode they mean that the waveguide mode can be thought of as being predominantly composed of two obliquely traveling TE surface waves as suggested on the left in Fig. 1(a), and analogously for "TM" modes. Their analysis shows that when a surface wave strikes a vertical edge at an oblique angle, the boundary conditions result in some conversion of the incident surface wave from its original wave type to the opposite wave type. As a result, the waves cannot be purely TE or purely TM in character, and in certain types of uniform dielectric waveguide structures leakage may exist which might not be expected from conventional points of view [2].

In [3], the analysis described above is extended to the case of dielectric waveguides with arrays of grooves added as suggested to the right in Fig. 1(a), and also wide gratings as in Fig. 1(b). (Gratings as in Fig. 1(a) are of potential interest for use in filters among other applications.) Let us for the moment consider the case of a wide grating with a single-wave incident as suggested in Fig. 1(b). If a lowest order TM mode is incident, the TM-to-TE conversion in the grating may result in the generation of an independent, lowest order TE bound mode in addition to the initial TM mode. Such a bound TE mode could be quite troublesome as it could have a phase velocity only slightly different from that of the incident TM wave, and it could create an unwanted, spurious, grating stopband quite close in frequency to the desired grating stopband.

In [4], an effect such as that described above is demonstrated experimentally for the case of a laser beam incident at an oblique angle onto a grating much wider than the incident beam as in Fig. 1(b). With a TE surface-wave beam incident, a stopband was observed due to the TE wave along with an overlapping, strong stopband due to the TM wave generated in the grating by

Manuscript received June 3, 1982; revised September 9, 1982. This research was supported by the National Science Foundation under Grant ECS-8016720. The author is with the Department of Electrical and Computer Engineering, University of California, Santa Barbara, CA 93106.

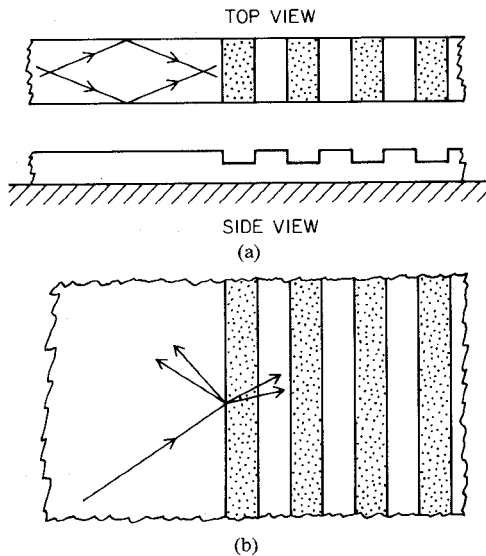


Fig. 1. (a) A dielectric image guide with a grating. (b) A wide grating with a single wave incident.

TE-to-TM mode conversion within the grating. It should be noted that this TE-to-TM mode conversion happens only when the beam is incident on the grating at an oblique angle. If the beam is incident normally on the grating there is no TE-to-TM mode conversion and no overlapping spurious stopband (though there could be some additional spurious stopbands at more separated frequencies due to TE-to-higher-order-TE mode conversions).

In [3], various dispersion diagrams are presented which clarify the various mode couplings which can occur when a wave is obliquely incident upon a grating. These numerous mode couplings are noted to be a source of difficulty for any potential use of dielectric waveguide gratings in filter components. Though [3] greatly clarifies the mode-coupling problems in grating structures, such as those in Figs. 1(a) and 1(b), it does not discuss an important distinction between these two cases.

It is the purpose of this note to observe that in the case of dielectric waveguides as in Fig. 1(a), the mode-coupling situation is not as bad as it is in the case of a single oblique wave as in Fig. 1(b). This is because in Fig. 1(a) there is symmetry present which does not exist in the case in Fig. 1(b). This symmetry causes mode selection which eliminates part of the mode couplings including the troublesome lowest order TM-to-TE (or TE-to-TM) mode couplings. Thus, dielectric waveguide gratings as in Fig. 1(a) have fewer mode coupling problems than one might expect in view of the problems associated with the case in Fig. 1(b).

## II. EFFECTS OF SYMMETRIES AND GROUND PLANES

In Fig. 1(a) there are symmetric pairs of incident waves which give the mode fields symmetry. Since only modes with the same type of symmetry can couple, these symmetries eliminate part of the couplings. Also, if the waveguide structure has a groundplane, it may in some cases help to separate mode resonances in frequency and thus give a wider band free of spurious responses. Let us consider the "image guide" examples in Fig. 2. We shall continue to call a mode TE or TM using the definitions in [1]–[3], but as in [5], we shall add double subscripts to help identify the mode. The first subscript will be the number of field variations in the  $x$  direction while the second subscript will be the number of field variations in the  $y$  direction. We will use arrows to suggest the nature of the dominant transverse  $E$ -field pattern for each mode. Fig. 2(a) shows the  $TM_{11}$  ( $EH_{11}$  in [5]) mode which is the

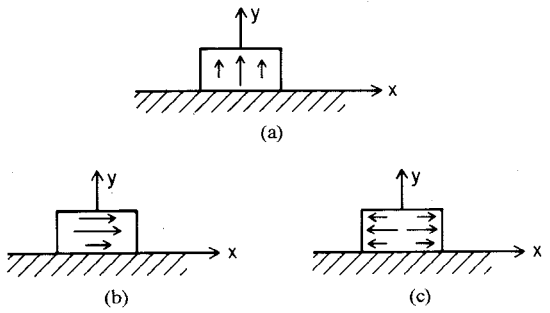


Fig. 2. Some pseudo TM and TE modes in dielectric image guide. The arrows suggest dominant  $E$ -field directions. (a)  $TM_{11}$  mode. (b)  $TE_{11}$  mode. (c)  $TE_{21}$  mode.

dominant mode and which has no cutoff frequency [5]. Fig. 2(b) suggests the lowest order TE mode which is the  $TE_{11}$  mode (the  $E_{11}^x$  mode in [6]). Due, in part, to the aspect ratio chosen for the guide, but largely due to the presence of the ground plane, this mode will have a quite appreciably higher phase velocity at a given frequency than will the  $TM_{11}$  mode (or the  $TE_{11}$  mode may be "cutoff"). Note that the  $E$  field will be mostly parallel to the ground plane, hence must go to zero at its surface. Also, the field variation is relatively cramped in the vertical direction. Both of these factors will tend to force a relatively large amount of the energy to be outside the dielectric and the phase velocity to be relatively high.

Observe that the  $TM_{11}$  mode has even symmetry in its  $E$  field in the  $x$  direction, but that the  $TE_{11}$  mode has odd symmetry<sup>1</sup> in that direction. Since the grating discontinuities preserve the symmetry in the  $x$  direction, any TM-to-TE mode conversions at the discontinuities must result in TE modes with even symmetry. Thus, the lowest order TE mode that could be generated is the  $TE_{21}$  mode<sup>1</sup> shown in Fig. 2(c) which has an even higher phase velocity (and cutoff frequency) than that of the  $TE_{11}$  mode. Thus, for this situation, any spurious stopbands resulting from TM-to-TE mode conversion will occur at frequencies well away from the desired TM-mode stopband. Any TM-to-higher-order-TM mode conversions must also result in  $E$  fields with even symmetry in the  $x$  direction, but can have any variation in the  $y$  direction. Thus, the  $TM_{11}$  mode cannot excite the  $TM_{21}$  mode which is odd symmetric in the  $x$  direction, but might excite either the  $TM_{31}$  or  $TM_{12}$  modes which are both even in the  $x$  direction. Probably in most cases the  $TM_{12}$  mode would be the one which could give a spurious stopband closest to the desired stopband. This appeared to be true in our experimental work described below for the case of an image-guide grating with notches in its top surface with a  $TM_{11}$  mode incident.

The experimental curve in Fig. 3 is consistent with the above conclusions. This is the transmission characteristic (an analogous reflection characteristic can be found in [7]) through a grating fabricated in image guide made of Rexolite 1422, 0.5 in wide and 0.4 in high with  $\epsilon_r = 2.55$ . The guide had 32, 3/32-in-deep notches in both of its sides. (The top side was left smooth.) The notches were 0.208 in long separated by 0.227 in. Both of these dimensions correspond to approximately a quarter guide wavelength at the stopband center frequency. The insertion loss in

<sup>1</sup>In Fig. 2(b), the fields have odd symmetry in the  $x$  direction in the sense that the fields on the left side of the  $y-z$  plane point into the plane while those on the right side of the  $y-z$  plane point out of the plane. Note that any  $E$  field fringing to the surface of the ground plane will be pointed down on the right side and up on the left side. Likewise in Fig. 2(c) the fields have even symmetry in the  $x$  direction in the sense that the fields on both sides of the  $y-z$  plane point out of the plane. Further, note that in this case any  $E$  field fringing to the ground plane will be pointed downward on both sides of the guide.

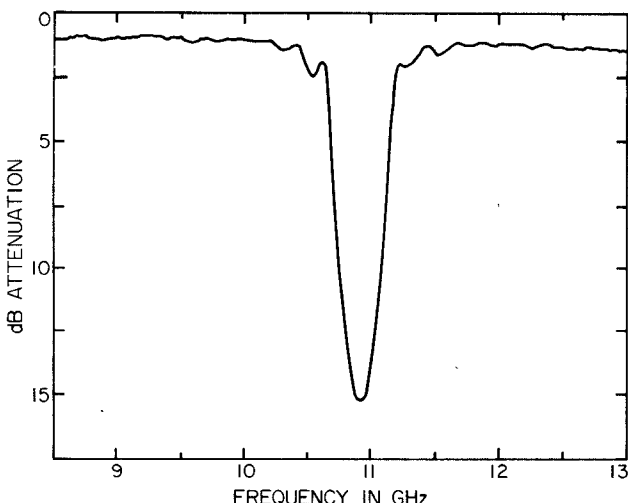


Fig. 3. Measured attenuation characteristics of a dielectric waveguide grating.

cludes the loss of the metal-guide-to-dielectric-guide transducers which have tapered dielectric guides in them, and about 7 in of uniform dielectric guide (which was mostly inside specially designed mode-launching horns mounted on top of the ground plane). The incident mode was  $TM_{11}$ . Note that unlike the responses in [4], no spurious stopband is present near the desired stopband. Tests were made up as far as 18 GHz with no spurious stopbands; but the transmission loss rose with more or less continuously increasing slope, reaching 10 dB by 18 GHz, because the grating was radiative at the higher frequencies.<sup>2</sup> If the grating had been made from a material with a higher dielectric constant, the grating could have been designed so as not to become radiative so soon, and probably spurious stopbands would have been evident at the higher frequencies due to mode conversions. Nevertheless, it appears that whether the adjacent higher frequencies are radiative or not, there can be a sizeable band about the desired stopband which is free of spurious responses or appreciable radiation.

In order to further confirm that no coupling can take place between lowest order TM and TE modes in this grating structure, the experimental setup was revised so as to launch the  $TE_{11}$  mode. This was done by orienting the terminating waveguides so that their  $E$  planes were parallel to the ground plane, and then introducing appropriate horns and dielectric waveguide tapers. In this case, the lowest and strongest stopband was centered at 12.39 GHz, and this should clearly be due to the  $TE_{11}$ -mode grating resonance. Note that the response in Fig. 3 shows no sign of a stopband at 12.39 GHz, which confirms that the  $TM_{11}$  mode launched when making the measurements in Fig. 3 was not coupling to the  $TE_{11}$  mode.

The measurements discussed above were all made using a dielectric image-guide grating made by cutting notches on both sides of the guide. Similar measurements were made on another grating formed by cutting notches in the top surface of the guide. This image guide again had  $\epsilon_r = 2.55$ , a 0.5-in width, and a 0.4-in height. The notches were 0.129 in deep, 0.227 in long, and were separated 0.208 in. When the  $TM_{11}$  mode was launched into this

grating a stopband was observed at 10.73 GHz, which should be the  $TM_{11}$ -mode resonance; and this was followed by a strong, broad stopband at 12.55 GHz. This second stopband should be due to a  $TM_{12}$ -mode resonance, since this mode has even symmetry and should be strongly coupled by the grating notches at the top of the guide. If there were coupling between the  $TM_{11}$  and  $TE_{11}$  modes in the grating, the second resonance could also be due to the  $TE_{11}$  mode. Next, the  $TE_{11}$  mode was launched into the grating, and a very strong stopband was observed centered at 12.82 GHz. Since this is a higher frequency than the frequency of the second stopband of the response when a  $TM_{11}$  mode was launched, it did not appear that the second stopband could have been due to coupling to a  $TE_{11}$ -mode resonance. To further confirm this, a metal plate was placed on top of the guide so it had two parallel ground planes with the guide between. Adding this plate should have relatively little effect on the frequency of a  $TM_{12}$ -mode resonance (since its  $E$  field is predominantly vertically polarized) while it should have a strong effect on the frequency of a  $TE_{11}$ -mode resonance (since its  $E$  field is predominantly parallel to the plates). When the structure was driven by the  $TM_{11}$  mode, both the first and second stopbands were very strong, and the frequency of the second stopband was virtually unchanged (which rules out the stopband being due to a  $TE_{11}$ -mode resonance). To further verify this last point, the structure was driven by the  $TE_{11}$  mode, and the  $TE_{11}$ -mode stopband was found to have moved from 12.82 GHz up to 14.26 GHz due to the addition of the metal cover plate. Thus, the second stopband observed when the grating with notches in its top was driven by  $TM_{11}$ -mode propagation could not have been due to mode conversion to a  $TE_{11}$  mode.

A possibly important fact was noted in the course of making the measurements outlined above. This is that the  $TM_{11}$  response of the grating had a much stronger stopband and was much more free of spurious responses for the case of grating notches cut in the sides of the guide, while, when the system was driven by the  $TE_{11}$  mode, the response was much superior for the guide with the grating notches cut in the top of the guide. Thus, at least for the gratings tested, if the  $TM_{11}$  mode is to be used, notches on both sides of the gratings are decidedly the best, while, if the  $TE_{11}$  mode is to be used, notches on the top of the image guide are decidedly the best.

In many filter applications it should be possible to work around the spurious responses or radiation that occur at higher frequencies so as to obtain a quite wide band of useful operation. For example, we have been working on some types of filters which use parallel-coupled grating resonators with a special absorbing load built into an end of each grating. These filters operate like reflection-type bandpass filters as long as the gratings are reflecting, but attenuate strongly by absorption at other frequencies. In this type of filter, radiation from the gratings at higher frequencies need not necessarily be harmful. (If desired, an absorptive cover plate can be used.) We found that a trial design of this type having a passband at 10 GHz maintained an uninterrupted stopband up at least as far as 18 GHz (which was as far as measurements were made). Some preliminary results from this work are discussed in [9]. Related results from another form of filter using coupled gratings are given in [10].

### III. CONCLUSIONS

The dielectric waveguide in Fig. 1(a) is seen to have fewer troublesome mode couplings than occurs for the single beam on a wide grating as shown in Fig. 1(b). The grating stopband characteristics in [7] and in Fig. 3 herein, and the bandpass filter results in [9] and [10], indicate that, though dielectric waveguide

<sup>2</sup>If we view the grating discontinuities as radiating elements with period  $d$ , then at 18 GHz,  $d/\lambda = 0.74$  (where  $\lambda$  is the free-space wavelength) while the phase shift per period in the guide is roughly  $-\pi/9$  rad. With these parameters uniform, linear array theory [8] predicts a nearly broadside major radiation lobe. In contrast, at the stopband at 10.9 GHz,  $d/\lambda = 0.45$  while the phase shift per period is  $-\pi$  rad. In this case, the so-called "visible region" is such that only weak "side lobes" are included in the radiation pattern.

gratings present certain problems, they can be useful in dielectric waveguide devices such as filters.

#### ACKNOWLEDGMENT

Thanks are due to Y. M. Kim, D. C. Park, and J. P. Duvall for making the various measurements described above.

#### REFERENCES

- [1] S.-T. Peng and A. A. Oliner, "Guidance and leakage properties of open dielectric waveguides: Part I—Mathematical formulations," *IEEE Trans. MTT Microwave Theory Tech.*, vol. MTT-29, pp. 843–855, Sept. 1981.
- [2] A. A. Oliner, S.-T. Peng, T.-I. Hsu, and A. Sanchez, "Guidance and leakage properties of open dielectric wave guides: Part II—New physical effects," *IEEE Trans. Microwave Theory Tech.*, vol. MTT-29, pp. 855–869, Sept. 1981.
- [3] M. J. Shau, H. Shigesawa, S.-T. Peng, and A. A. Oliner, "Mode conversion effects in Bragg reflection from periodic grooves in rectangular dielectric image guide," in *1981 Int. Microwave Symp. Dig.*, pp. 14–16, Cat. No. 81CH1592-5, IEEE, New York.
- [4] K. Wagatsuma, H. Sakaki, and S. Saito, "Mode conversion and optical filtering of obliquely incident waves in corrugated waveguide filters," *IEEE J. Quantum Electron.*, vol. QE-15, pp. 632–637, July 1979.
- [5] K. Solbach and I. Wolff, "The electromagnetic fields and the phase constants of dielectric image lines," *IEEE Trans. Microwave Theory Tech.*, vol. MTT-26, pp. 266–274, Apr. 1978.
- [6] S. Shindo and T. Itanami, "Low-loss rectangular dielectric image line for millimeter-wave integrated circuits," *IEEE Trans. Microwave Theory Tech.*, vol. MTT-26, pp. 747–751, Oct. 1978.
- [7] T. Itoh, "Applications of gratings in a dielectric waveguide for leaky-wave antennas and band-reject filters," *IEEE Trans. Microwave Theory Tech.*, vol. MTT-25, pp. 1134–1138, Dec. 1977.
- [8] R. E. Collin and F. J. Zucker, *Antenna Theory*, Part I. New York: McGraw-Hill, 1969, sec. 5.4.
- [9] G. L. Matthaei, C. E. Harris, D. C. Park, and Y. Kim, "Dielectric-waveguide filters using parallel-coupled grating resonators," *Electron. Lett.*, vol. 18, pp. 509–510, June 10, 1982.
- [10] G. L. Matthaei, C. E. Harris, Y. M. Kim, D. C. Park, and J. P. Duvall, "Simple dielectric waveguide band-pass filter," *Electron. Lett.*, vol. 18, pp. 798–799, Sept. 2, 1982.

## Temperature Stabilization of GaAs MESFET Oscillators Using Dielectric Resonators

CHRISTOS TSIRONIS, MEMBER, IEEE, AND VLAD PAUKER

**Abstract**—A simple model of the temperature stabilization of dielectric resonator FET oscillators (DRO's) is presented. Deduced from the oscillation condition, the model furnishes relations for oscillation power and frequency stability with temperature.

A stack resonator with an appropriate linear resonance frequency/temperature characteristic has been developed and used to stabilize a DRO: frequency stability of  $\pm 120$  kHz over  $-20^\circ\text{C}$  to  $80^\circ\text{C}$  ( $\triangle \pm 0.1$  ppm/K) at 11.5 GHz has been achieved.

#### I. INTRODUCTION

The availability of highly stable low-loss dielectric material has led to the development of a family of microwave solid-state signal sources: the dielectric resonator oscillators (DRO's).

The frequency stability with temperature of a GaAs FET DRO with the dielectric resonator coupled as a band rejection filter at

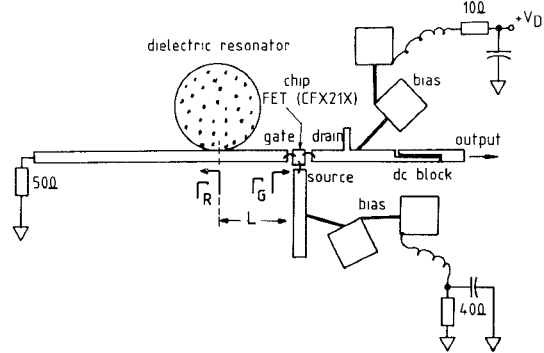


Fig. 1 Layout of FET dielectric resonator stabilized oscillator.

the output port has been analyzed in [1] and for a Gunn-diode DRO in [2]. However, the highest stability with temperature has been reported in [3] for a reflection type FET DRO.

It is the aim of this paper to present an approach to temperature stability modeling of DRO's different from those described in [1], [2] and resulting in a model that furnishes concepts and limits for frequency stabilization, oscillation power, and requirements for an optimum resonator material. As an example, a very stable DRO with a GaAs FET chip from RTC (CFX 21 X) will be presented.

#### II. STABILIZATION MODEL

The reflection type FET DRO treated in our analysis is shown in Fig. 1. It is a common source configuration with capacitive series feedback that presents at the gate port a negative impedance

$$Z_G = -R_G + \frac{1}{j\omega C_G}$$

corresponding to the reflection coefficient

$$\Gamma_G = |\Gamma_G| \cdot e^{j\varphi_G} \quad \text{with } |\Gamma_G| > 1.$$

From this point of view, the analysis is valid for any DRO circuit that can be described this way. The impedance of a matched microstrip line coupled with a dielectric resonator (Fig. 1) can be calculated at the plane of the resonator as

$$Z_R = Z_0 + Z_0 \cdot \beta / \left( 1 + 2j \cdot \frac{f - f_r}{f_r} Q_r \right). \quad (1)$$

The corresponding reflection coefficient is

$$\Gamma_R = \beta / \left( 2 + \beta + 4j \cdot \frac{f - f_r}{f_r} \cdot Q_r \right) \quad (2)$$

with  $\beta$  the coupling factor between dielectric resonator and microstrip line,  $f_r$  and  $Q_r$  the resonance frequency and unloaded  $Q$ -factor of the dielectric resonator when coupled to the microstrip line, and  $Z_0$  the characteristic impedance of the line. At the plane of the FET,  $\Gamma_R$  appears transformed by the microstrip line  $L$  to

$$\Gamma'_R = \Gamma_R \cdot e^{-j\tau f} \quad \text{with } \tau \approx 1.07 \cdot L \cdot 10^{-10} \text{ s/mm.} \quad (3)$$

The oscillation condition is now applied at the plane of the gate port

$$\Gamma'_R \cdot \Gamma_G = 1 \quad (4)$$

Manuscript received June 7, 1982; revised September 9, 1982.  
The authors are with Laboratoires d'Electronique et de Physique Appliquée, 3 Avenue Descartes, 94450 Limeil-Brevannes, France.